Optimal Model Complexity in Geological Carbon Sequestration: A Design of Experiment (DoE) & Response Surface (RS) Uncertainty Analysis

Project Number: DE-FE-0009238

Mingkan Zhang[1], Ye Zhang[1], Peter Lichtner[2]

1.Dept. of Geology & Geophysics, University of Wyoming, Laramie, Wyoming
2.OFM Research, Inc., Santa Fe, New Mexico

U.S. Department of Energy
National Energy Technology Laboratory
Carbon Storage R&D Project Review Meeting
Developing the Technologies and
Infrastructure for CCS
August 18-20, 2015

Presentation Outline

- Project goals and benefits;
- Detailed project objectives & success criteria;
- Accomplishments to date;
- Summary of results;

Benefit to the Program

Major goals:

Support industry's ability to predict CO_2 storage capacity in geologic formations to within ±30% accuracy;

Develop and validate technologies to ensure 99% storage permanence.

Project benefits:

Facilitate the development and implementation of efficient workflows for modeling field-scale GCS in a variety of geochemically reactive environments, where formations exhibit multiple scales of permeability (*k*) heterogeneity.

Project Overview:
Goals and Objectives

- Develop, test, and verify the DoE and RS uncertainty analysis for a fully heterogeneous reference model (FHM) & increasingly lower resolution “geologic models” created from upscaling the FHM.

- Investigate the effect of increasing reservoir *k* variance and depth on the uncertainty outcomes including optimal heterogeneity resolution(s). At greater injection depths, investigate gravity-stable injection.

- Investigate the effect of mineral reactions on GCS, including mineral volume fractions, reactive rate constants, reactive surface areas, and the impact of different geochemical databases.

Project Overview: Success Criteria

- At increasing depth, for both weakly and strongly heterogeneous systems, the geologic models can capture the FHM CO_2 behaviors; → Reduced characterization cost;

- RS analytical models are successfully verified against full-physics reservoir simulations via HPC, thus prediction uncertainty of any outcome at any time can be assessed using the low-resolution model(s) running the efficient RS models. → Enhanced computation efficiency;

- Mineral storage analysis: seeking the most efficient composition for reactive storage → Enhanced storage;

- Greater injection depth: within the uncertainty analysis framework, identify the combination(s) of favorable parameters & reservoir conditions that give rise to gravity-stable flow. → Enhanced storage security.

Accomplishments to Date

- High-resolution reservoir *k* heterogeneity (3.2 M grid cells) & geologic (upscaled) models of decreasing *k* resolutions built;
- For multiple system ln*k* variances, permeability upscaling & single-phase flow verification;
- For multiple system ln*k* variances, dispersivity upscaling & verification;
- Parallel simulation of CO_2 storage with PFLOTRAN & performance scaling on supercomputer;
- Uncertainty analysis of dissolution storage and CO_2 leakage in heterogeneous and the geologic models;
- Uncertainty analysis of CO_2 modeling considering mineral reactions;
- Uncertainty analysis of CO_2 modeling in greater injection depths.

Sediment Experiment at SAFL

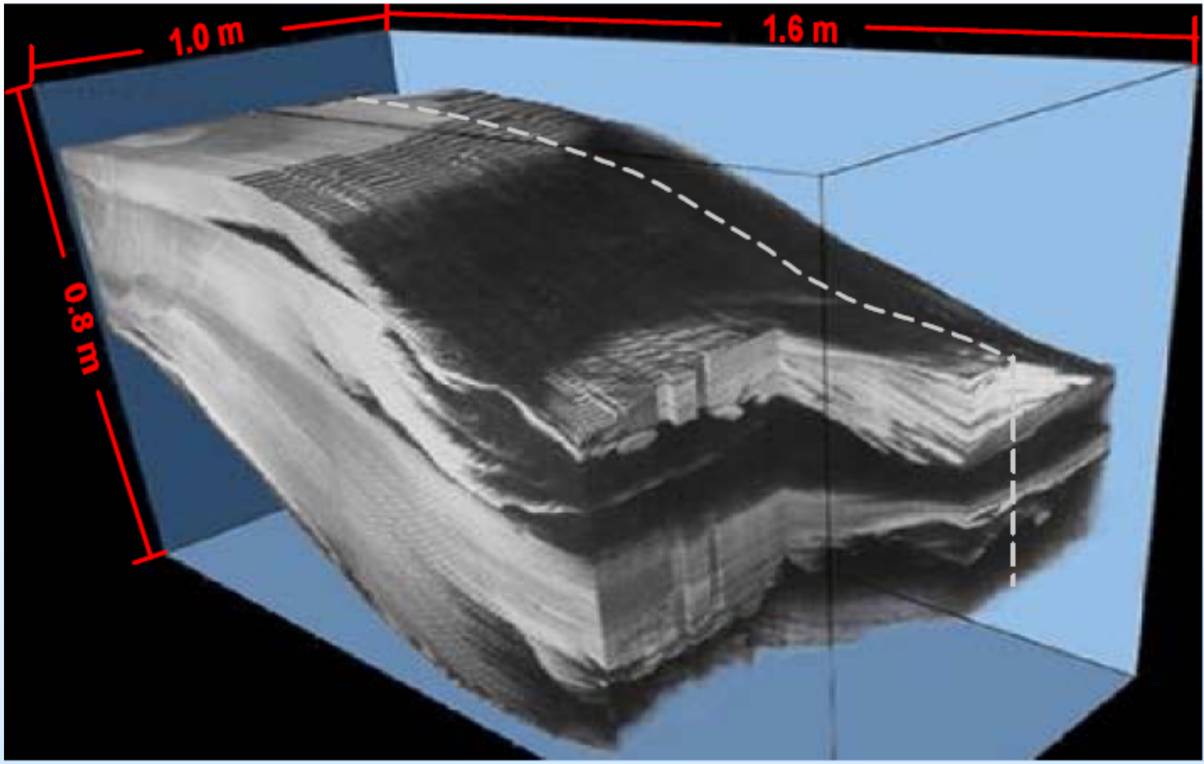

http://www.safl.umn.edu/

Project Leader: Prof. Chris Paola

Founding: NSF & oil industry consortium

Reservoir Heterogeneity Vs Geologic Models

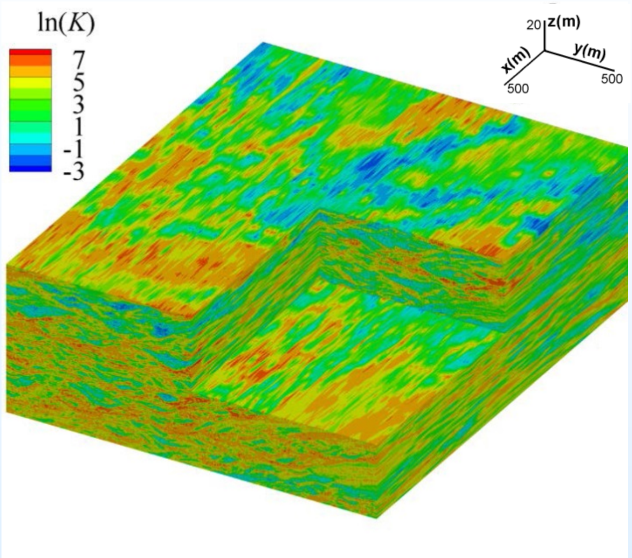

FHM

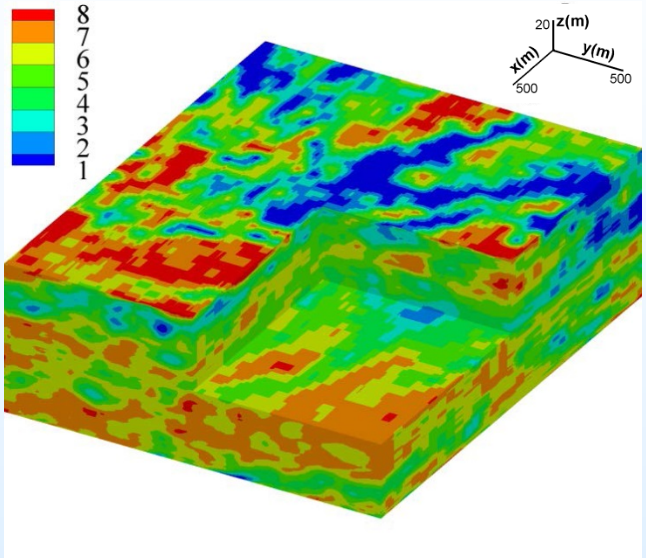

8-unit facies model

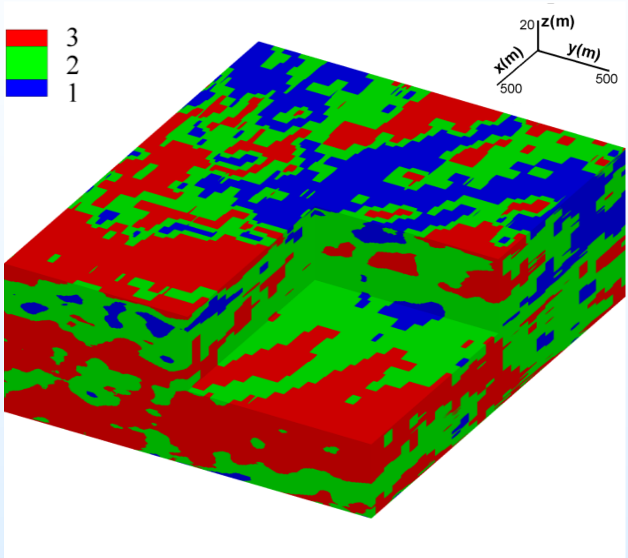

3-unit facies model

A 1-unit homogeneous “formation” model is also created (not shown);

Permeability Upscaling & Verification

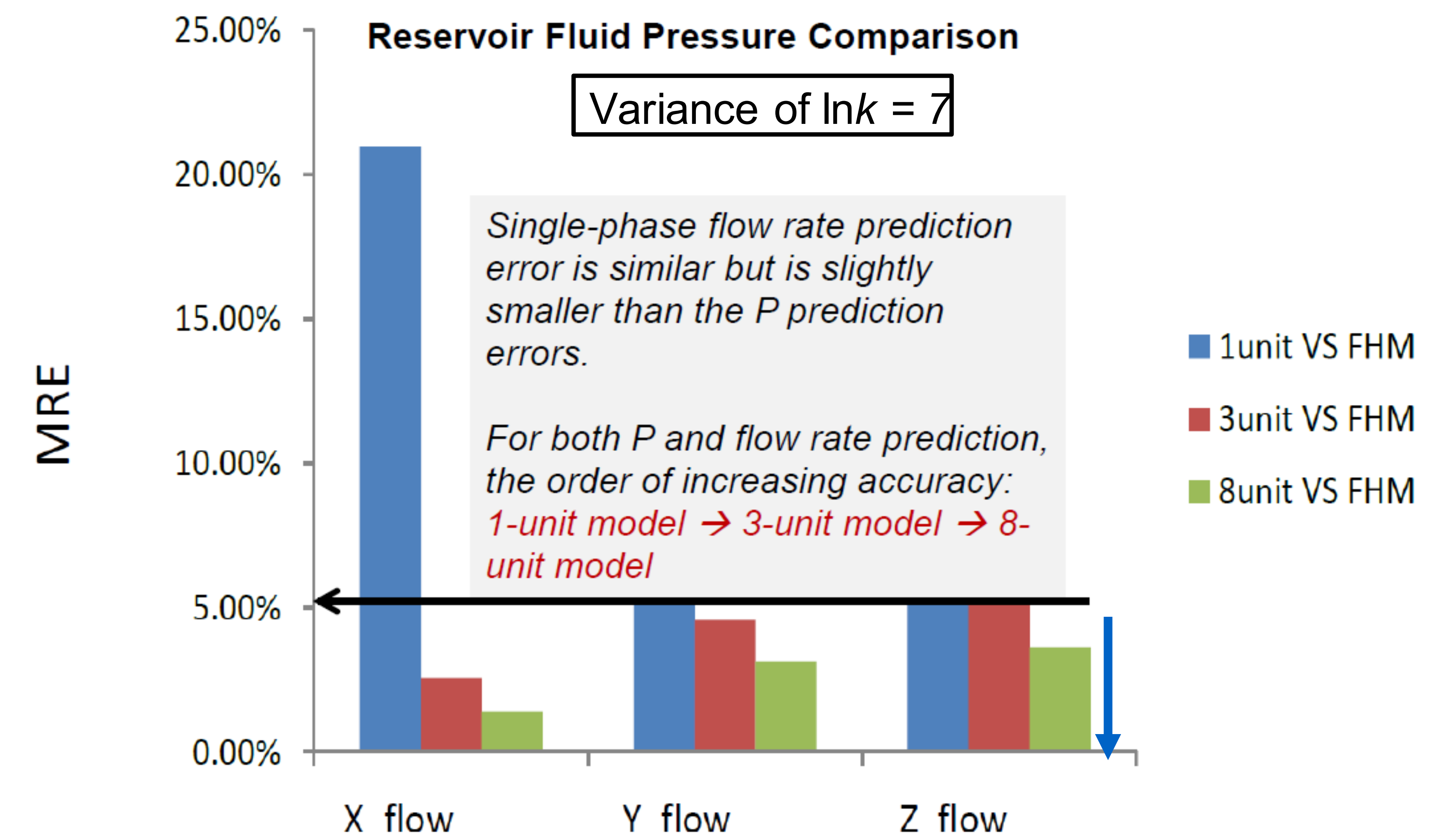

Dispersivity Upscaling & Verification

The plume moments are employed to compare the transport upscaling results as shown in Figure 3. The zero, first and second plume moments are defined as:

$$M = \iiint_{\Omega} (\theta c) dxdydz, \mathbf{L}_p = \frac{1}{M} \iiint_{\Omega} (\mathbf{X}_p \theta c) dxdydz \quad \text{and} \quad s^2 = \frac{1}{M} \iiint_{\Omega} (\mathbf{X}_p - \mathbf{L}_p)(\mathbf{X}_p - \mathbf{L}_p) \theta c dxdydz.$$

In addition, both the tailing behavior (Figure 4) and the breakthrough curve (Figure 5) of the FHM have been captured when the variance of ln(*K*) is low to modest.

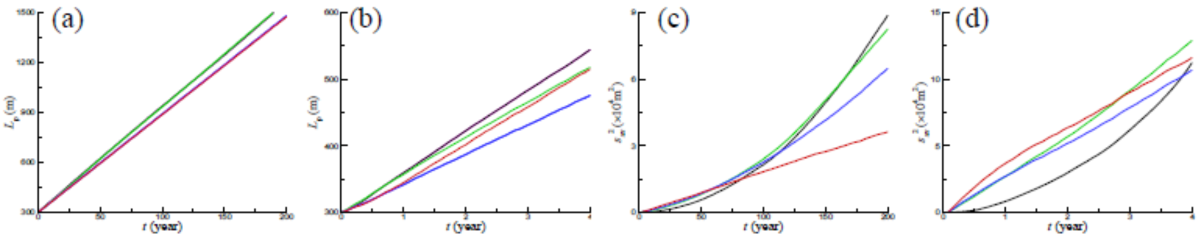

Figure 3. Evolution of plume moments with time: (a) & (b) mean plume displacements for variance(ln*K*) = 0.1 and 4.5, respectively; (c) & (d) longitudinal plume covariances for variance(ln*K*) = 0.1 and 4.5, respectively. The black, red, blue and green lines represent FHM, 1-unit, 3-unit and 8-unit models, respectively.

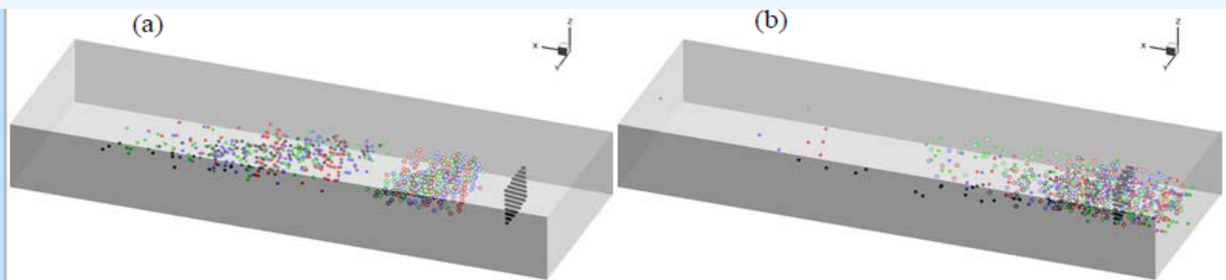

Figure 4. Particle locations in the simulation domain with (a) variance(ln*K*) = 0.1, and (b) variance(ln*K*) = 4.5. The black, red, blue and green points represent particles from the FHM, 1-unit, 3-unit and 8-unit models, respectively. The squares consisting of black points represent initial position. The empty and the filled cycles indicate particles at time 60 years and 180 years for (a) and 1.28 years and 3.84 years for (b). Only 100 particles are shown in one time step.

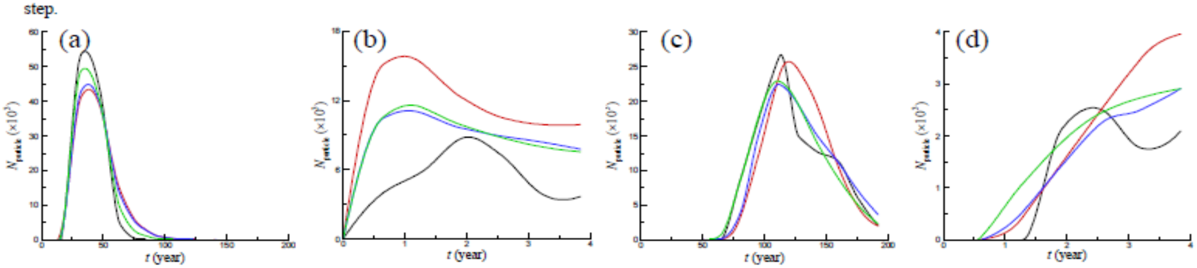

Figure 5. Breakthrough curve: (a) & (b) at *x* = 500m for variance(ln*K*) = 0.1 and 4.5, respectively; (c) & (d) at *x* = 1000m for variance(ln*K*) = 0.1 and 4.5, respectively. The black, red, blue and green lines represent FHM, 1-unit, 3-unit and 8-unit models, respectively.

- For a given variance, accuracy: 8-unit > 3-unit > 1-unit model;
- For var(ln*k*) up to 4.5, 8- and 3-unit models can accurately capture plume migration pathway, mass centroid, and size; Optimal resolution: 3-unit model.
- For var(ln*k*) = 0.1, all models can accurately capture solute transport BTC; Optimal resolution: 1-unit model.
- For var(ln*k*) = 4.5, only the 8-unit model can capture some aspect of solute transport BTC; Optimal resolution: 8-unit or higher.
- **Optimal heterogeneity depends on prediction goal and system variance.**

PFLOTRAN Scaling on Yellowstone

Yellowstone is a 1.5-petaflops supercomputer with 72,288 processor cores & 144.6 TB of memory.

http://www2.cisl.ucar.edu/resources/yellowstone

1-unit model (3.2M):

* *20 yr CO_2 injection + 2000 yr monitoring*
* *2048 cores*: 9 hours

1-unit model (25 M): CO_2 injection w/ reactive chemistry

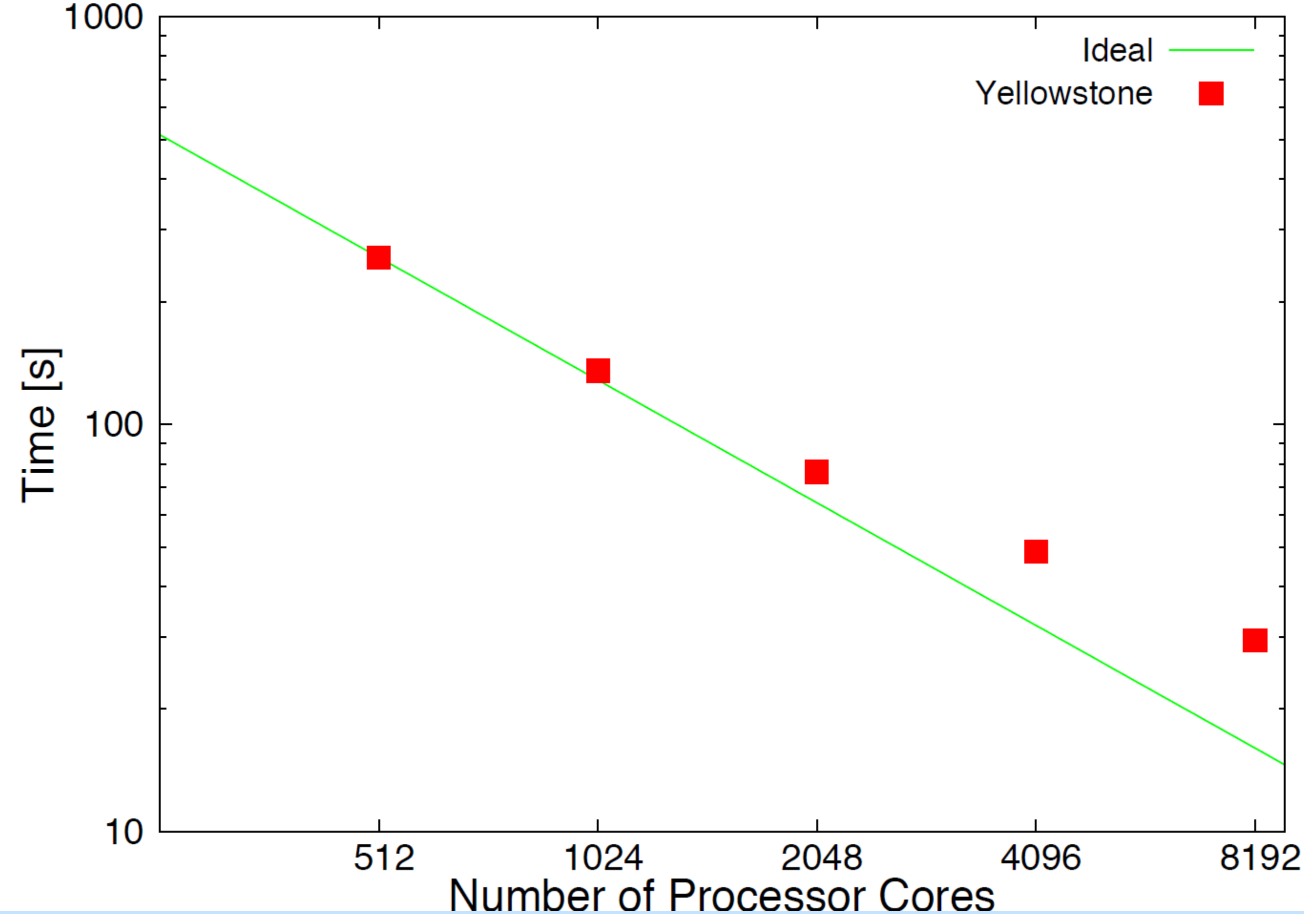

Uncertainty Analysis: CO_2 Storage & Leakage

Case	T Gradient (°C/m)	Brine Salinity (Molal)	k_{cap} (m^2)	Inject rate (kg/s)
1	-0.025	0	$10^{-17.5}$	4
2	-0.025	4	$10^{-17.5}$	4
3	-0.05	0	$10^{-17.5}$	4
4	-0.05	4	$10^{-17.5}$	4
5	-0.0375	2	10^{-16}	2
6	-0.0375	2	10^{-16}	8
7	-0.0375	2	10^{-19}	2
8	-0.0375	2	10^{-19}	8
9	-0.025	2	$10^{-17.5}$	2
10	-0.025	2	$10^{-17.5}$	8
11	-0.05	2	$10^{-17.5}$	2
12	-0.05	2	$10^{-17.5}$	8
13	-0.0375	0	10^{-16}	4
14	-0.0375	0	10^{-19}	4
15	-0.0375	4	10^{-16}	4
16	-0.0375	4	10^{-19}	4
17	-0.025	2	10^{-16}	4
18	-0.025	2	10^{-19}	4
19	-0.05	2	10^{-16}	4
20	-0.05	2	10^{-19}	4
21	-0.0375	0	$10^{-17.5}$	2
22	-0.0375	0	$10^{-17.5}$	8
23	-0.0375	4	$10^{-17.5}$	2
24	-0.0375	4	$10^{-17.5}$	8
25	-0.0375	2	$10^{-17.5}$	4

$scCO_2$ plume footprint

Time = 2K years (inj rate= 4kg/s; injection time = 10 years):

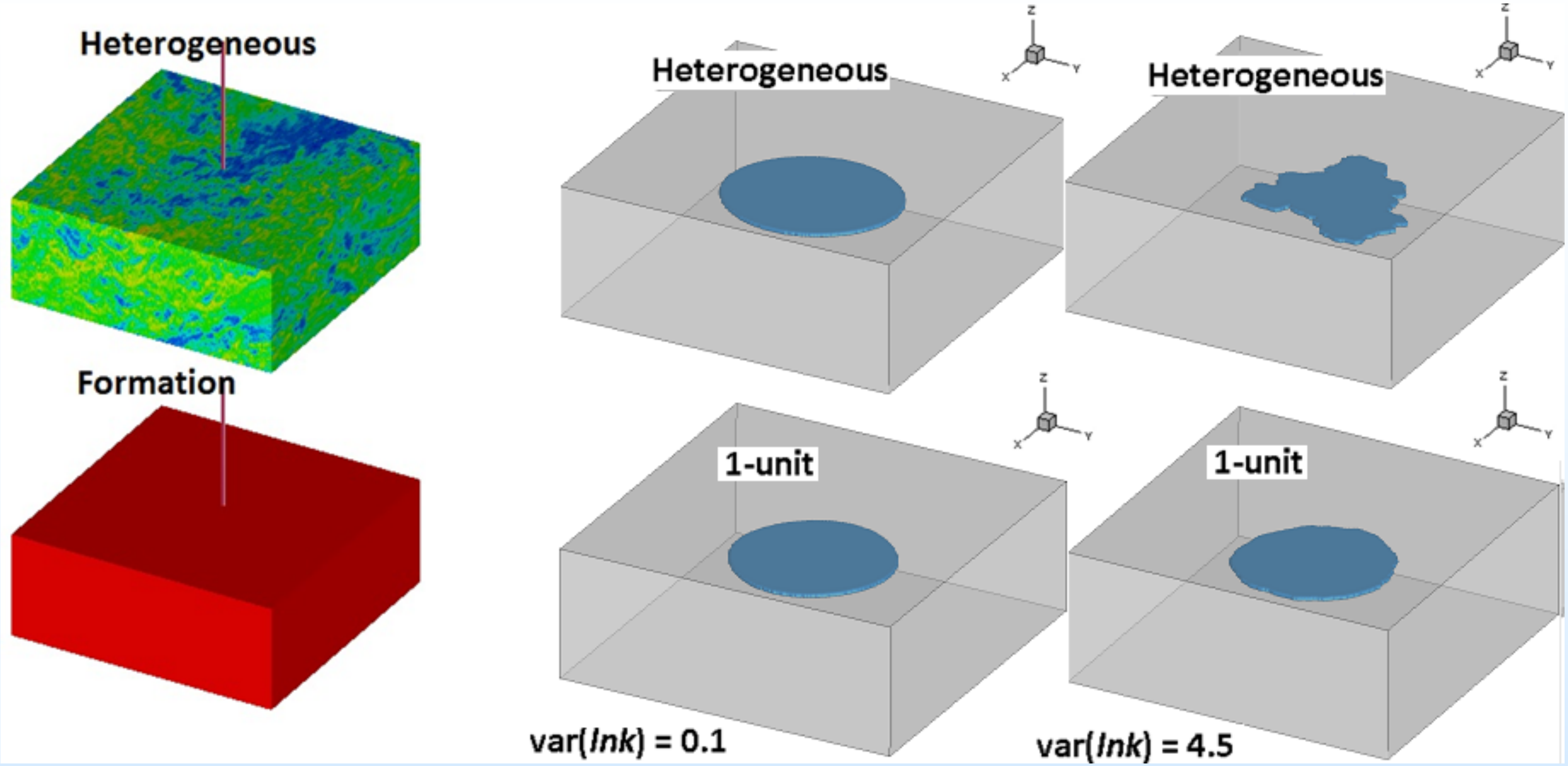

- When system *k* variance is low, the 1-unit model can accurately capture the $scCO_2$ plume footprint of the FHM.
- 8-unit and 3-unit models provide more accurate $scCO_2$ plume predictions than the 1-unit model, when system *k* variance is high,

Dissolved CO_2 Plume

Time = 2K years (inj rate= 4kg/s; injection time = 10 years):

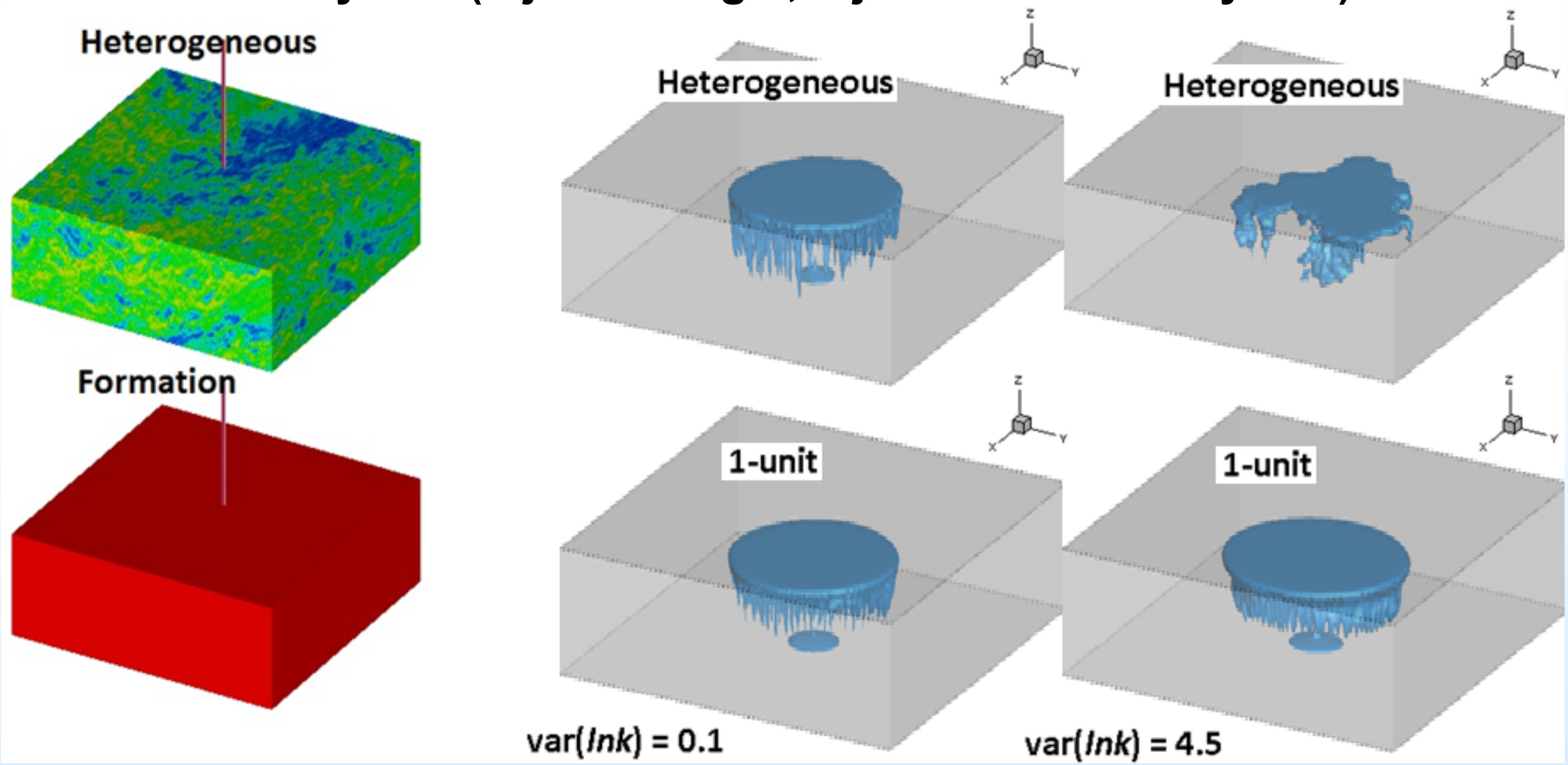

- When system *k* variance is low, the 1-unit model can accurately capture the dissolved CO_2 plume of the FHM.
- 8-unit and 3-unit models provide more accurate dissolved CO_2 plume predictions than the 1-unit model.

Dissolved CO_2

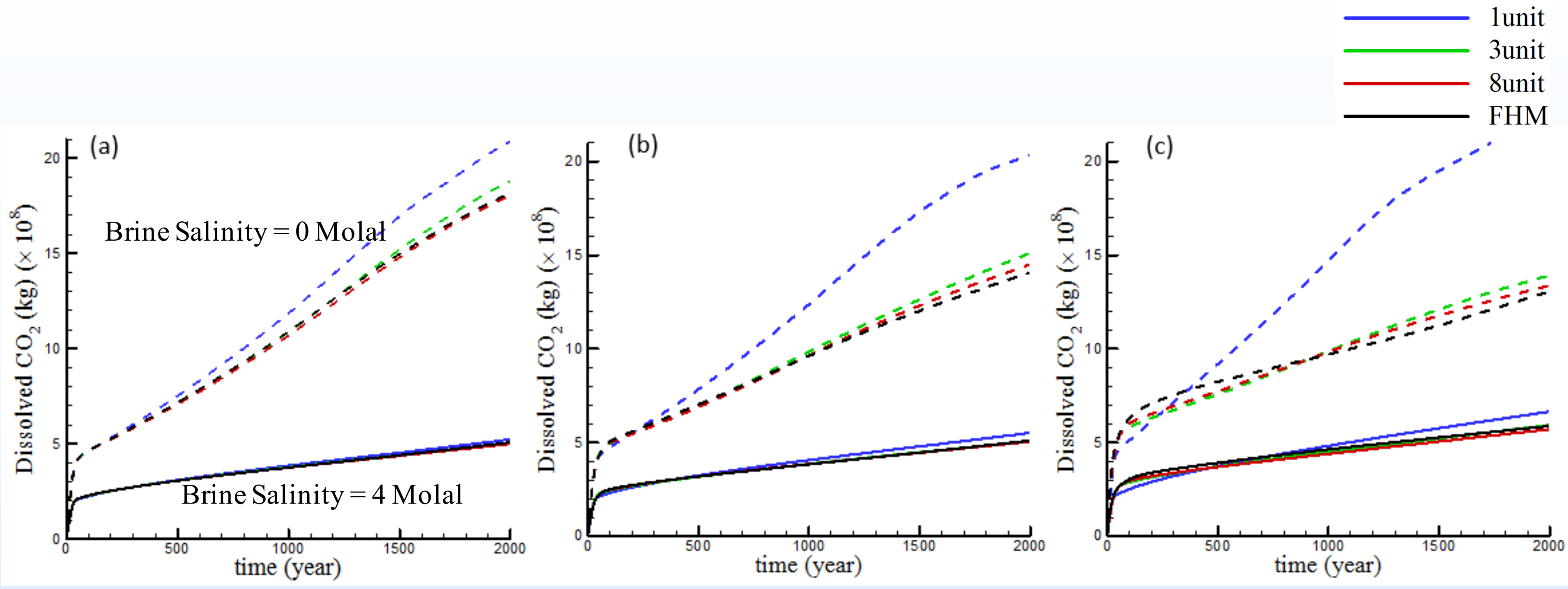

Var(ln*k*) = 0.1   Var(ln*k*) = 1.0   Var(ln*k*) = 4.5

- Increasing brine salinity decreases CO_2 dissolution.
- The 8-unit and 3-unit models yield great accurate dissolved CO_2 predictions.

Dissolved CO_2 at 2000 Years

	$\sigma^2 = 0.1$			$\sigma^2 = 1.0$			$\sigma^2 = 4.5$		
Model	Term	Scaled Estimate	Plot Estimate	Term	Scaled Estimate	Plot Estimate	Term	Scaled Estimate	Plot Estimate
1unit	T Gradient	-66525.68		T Gradient	1555.4917		T Gradient	-50947.11	
	Brin Salinity	-17979466		Brin Salinity	-17082310		Brin Salinity	-18280660	
	K Cap	1497108		K Cap	1860613		K Cap	1969252	
	Inj rate	287260.65		Inj rate	241458.07		Inj rate	-104160.2	
3unit	T Gradient	-32093.85		T Gradient	27034.642		T Gradient	17782.292	
	Brin Salinity	-15783477		Brin Salinity	-11537619		Brin Salinity	-9257227	
	K Cap	1460367		K Cap	1767155		K Cap	1770883	
	Inj rate	410148.22		Inj rate	421509.17		Inj rate	-82521.86	
8unit	T Gradient	16158.892		T Gradient	48589.475		T Gradient	60138.433	
	Brin Salinity	-14915585		Brin Salinity	-10880135		Brin Salinity	-8878195	
	K Cap	1776827		K Cap	1745176		K Cap	1735825	
	Inj rate	340980.92		Inj rate	450741.17		Inj rate	426151.34	
FHM	T Gradient	14264.942		T Gradient	39376.7		T Gradient	-6628.533	
	Brin Salinity	-14967318		Brin Salinity	-10393509		Brin Salinity	-8334250	
	K Cap	1765641		K Cap	1687305		K Cap	1611689	
	Inj rate	320034.78		Inj rate	488939.2		Inj rate	544649.55	

Leakage of CO_2 into caprock

Time = 2K years (inj rate= 4kg/s; injection time = 10 years):

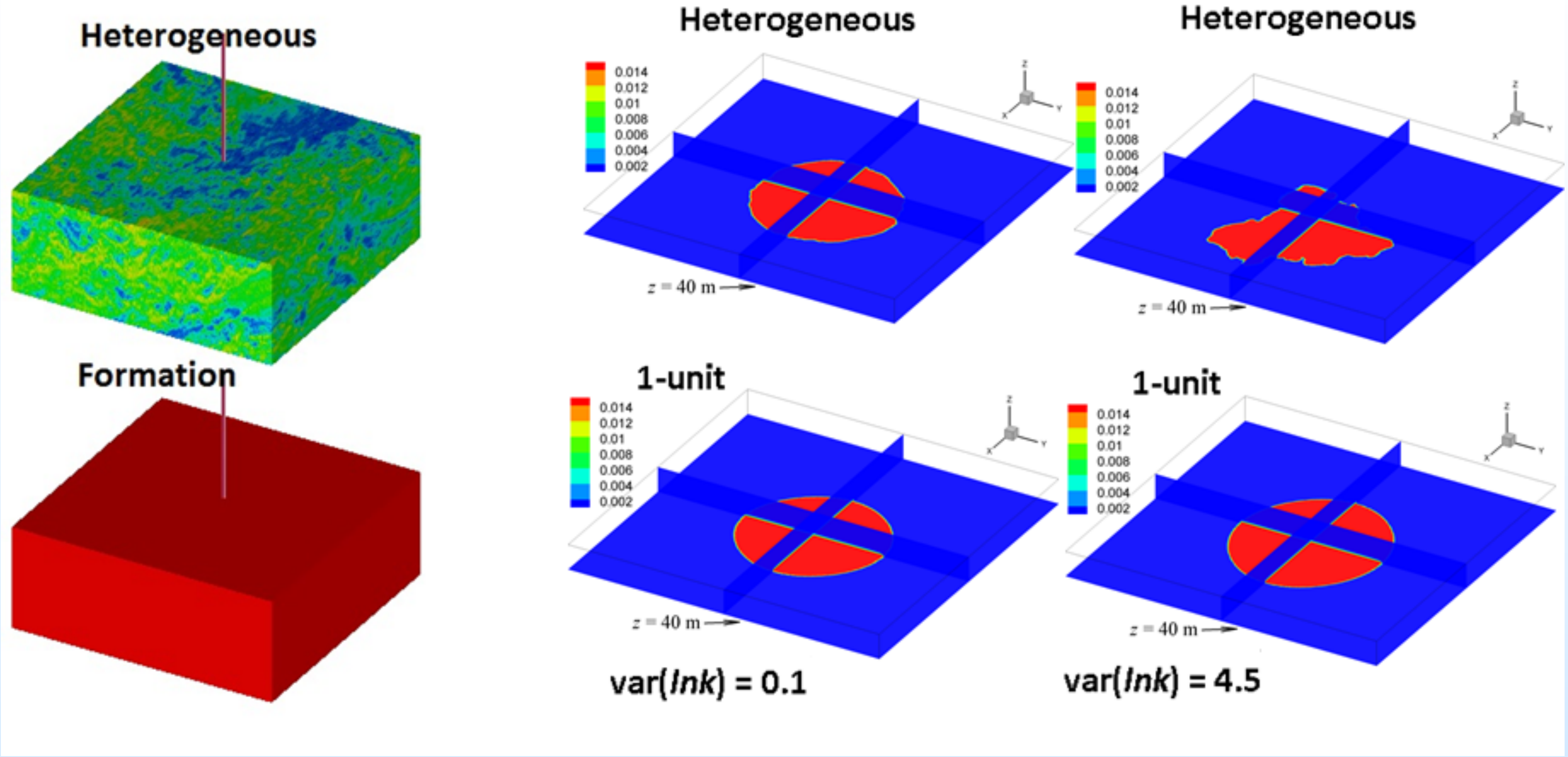

- Under low variance condition, the 1-unit model can reasonably capture the leakage plume of the FHM.
- The 8-unit and 3-unit models yield more accurate leaked CO_2 plume predictions than the 1-unit model.

Leakage of CO_2 into caprock

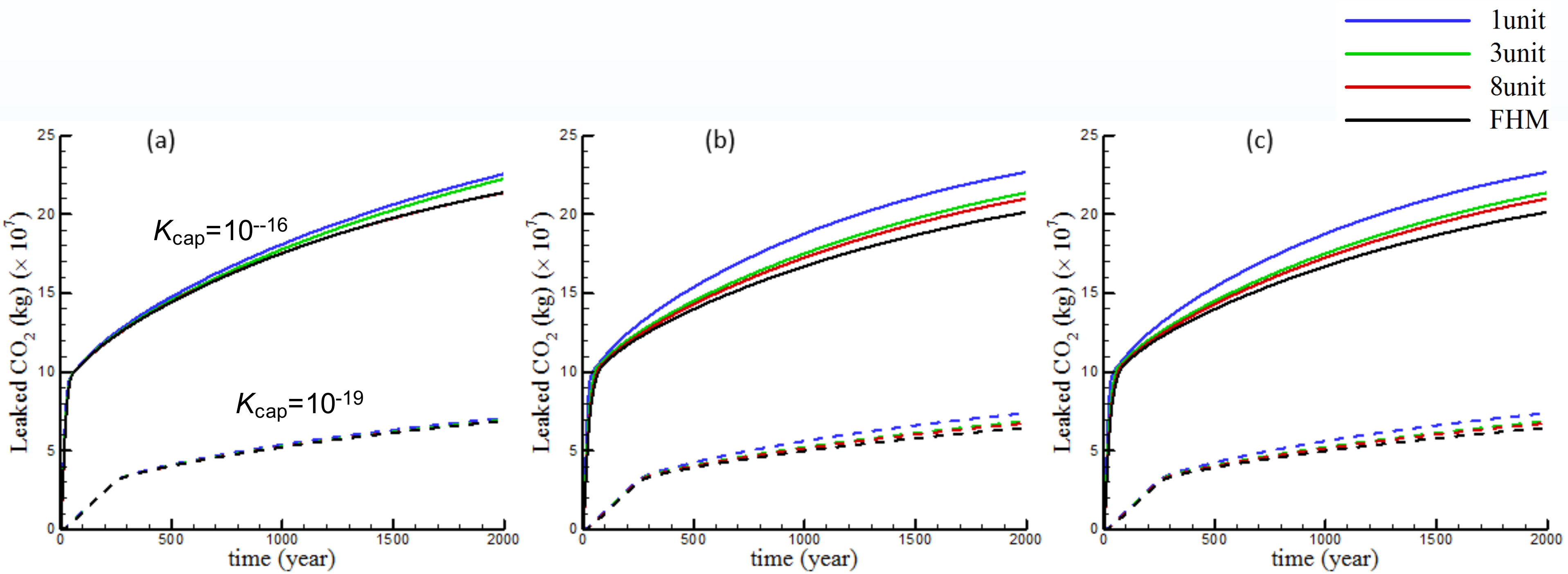

Var(ln*k*) = 0.1

Var(ln*k*) = 1.0

Var(ln*k*) = 4.5

- The decreasing caprock permeability reduces CO_2 leakage.
- Base on results of the upscaling study, the 8-unit and 3-unit models yield great accurate Leaked CO_2 predictions.

Uncertainty Results for CO_2 Leakage

	$\sigma^2 = 0.1$			$\sigma^2 = 1.0$			$\sigma^2 = 4.5$		
Model	Term	Scaled Estimate	Plot Estimate	Term	Scaled Estimate	Plot Estimate	Term	Scaled Estimate	Plot Estimate
1unit	T Gradient	469420.96		T Gradient	-388487.8		T Gradient	-1419857	
	Brin Salinity	-15384250		Brin Salinity	-14242776		Brin Salinity	-8039491	
	K Cap	-76663063		K Cap	73456018		K Cap	81043291	
	Inj rate	-2662427		Inj rate	-3308578		Inj rate	-3977240	
3unit	T Gradient	543991.63		T Gradient	-194952.5		T Gradient	-544753.2	
	Brin Salinity	-18842939		Brin Salinity	-21237658		Brin Salinity	-20641268	
	K Cap	-76407790		K Cap	70965164		K Cap	75600868	
	Inj rate	-2558673		Inj rate	-2872086		Inj rate	-4702174	
8unit	T Gradient	-283710.1		T Gradient	-108156.7		T Gradient	-162012.8	
	Brin Salinity	-19111777		Brin Salinity	-21175701		Brin Salinity	-20683088	
	K Cap	-70108544		K Cap	69845490		K Cap	72073598	
	Inj rate	-2376895		Inj rate	-2710601		Inj rate	-4294708	
FHM	T Gradient	-307085.2		T Gradient	-91501.07		T Gradient	121540.03	
	Brin Salinity	-19035197		Brin Salinity	-20825214		Brin Salinity	-20438426	
	K Cap	-70111854		K Cap	67276691		K Cap	64498465	
	Inj rate	-2453283		Inj rate	-2954034		Inj rate	-3344799	

Mineral Storage Modeling

Mineral	Formula	Init VF (%)
Quartz	SiO_2	43.04
Calcite	$CaCO_3$	4.22
K-Feldspar	$KAlSi_3O_8$	15.77
Kaolinite	$Al_2Si_2O_5(OH)_4$	0
Albite	$NaAlSi_3O_8$	0
Plagioclase	$(Na_{0.75},Ca_{0.25})(Al_{1.25},Si_{2.75})O_8$	4.07
Illite	$K_{0.6}(Mg_{0.25}, Al_{1.8})(Al_{0.5}, Si_{3.5})O_{10}(OH)_2$	4.01
Hematite	Fe_2O_3	1.60
Dawsonite	$NaAlCO_3(OH)_2$	0
Chlorite	$(Mg_{2.5}, Fe_{2.5}, Al)(Al, Si_3)O_{10}(OH)_8$	7.19
Siderite	$FeCO_3$	0
Ankerite	$Ca(Mg_{1.3}, Fe_{0.7})(CO_3)_2$	0
Magnesite	$MgCO_3$	0
Na-Smectite	$Na_{0.290}(Mg_{0.26}, Al_{1.74})(Al_{0.03}, Si_{3.97})O_{10}(OH)_2$	0
Ca-Smectite	$Ca_{0.145}(Mg_{0.26}, Al_{1.74})(Al_{0.03}, Si_{3.97})O_{10}(OH)_2$	0
Dolomite	$(CaMg)(CO_3)_2$	0

Kihm et al. JOURNAL OF GEOPHYSICAL RESEARCH, 2012

Changes in Volume Fraction after 2000 Years

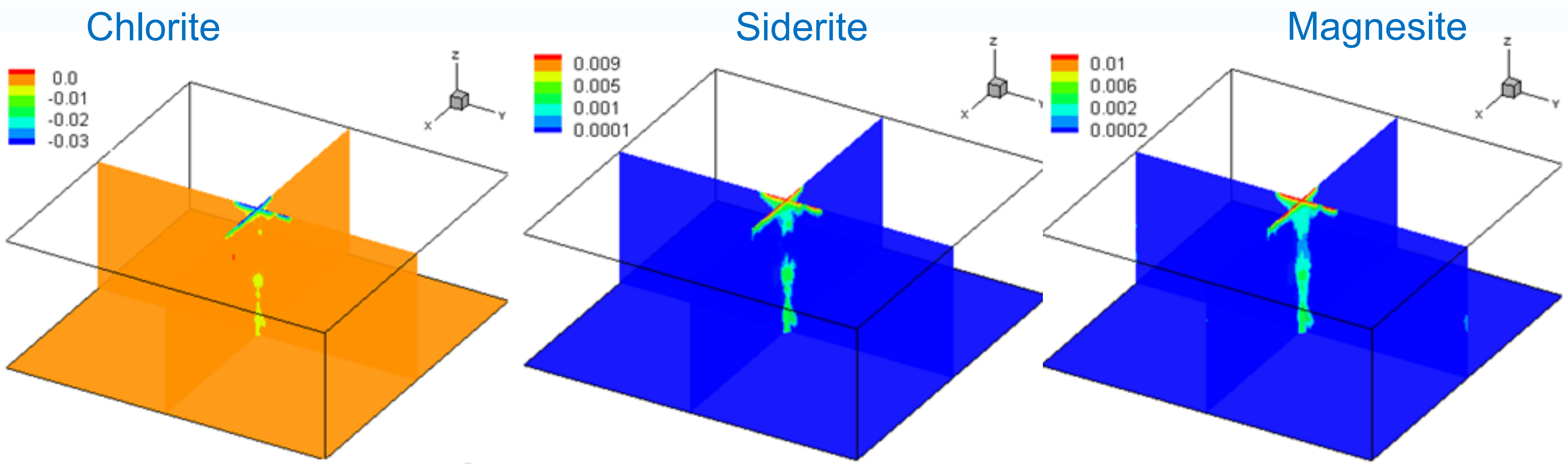

- Reactive minerals in sandstone such as Chlorite can provide cations such as Mg^{2+} and Fe^{2+}, which are essential chemical components for forming carbonate precipitates during GCS.
- The reactions between cations and CO_2 forms carbonate minerals (e.g., siderite, magnesite and ankerite) to trap CO_2 as precipitates.
- Uncertainty analysis evaluating important uncertainty factors is ongoing.

Deep Injection

- Deep injection trapping of CO_2 in deep marine sediments provides additional storage to existing onshore capacity.

- CO_2 can be trapped through 'self-sealing' gravitational and hydrate-forming mechanisms under suitable temperature and pressure conditions.

- Uncertainty analysis of ocean storage in the Gulf of Mexico is about sediment property, thermal gradient, sea water depth, etc.

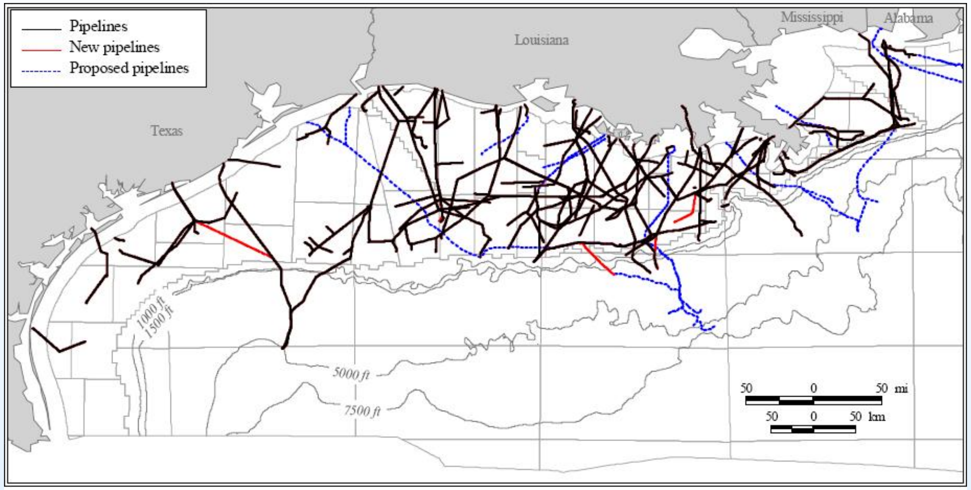

Figure 22. Oil and gas pipelines with diameters greater than or equal to 20 inches.

oil and gas pipe line in GOM (Richardson et al., 2004, OCS Report MMS 2004-021)

$scCO_2$ plumes at 1km water depth

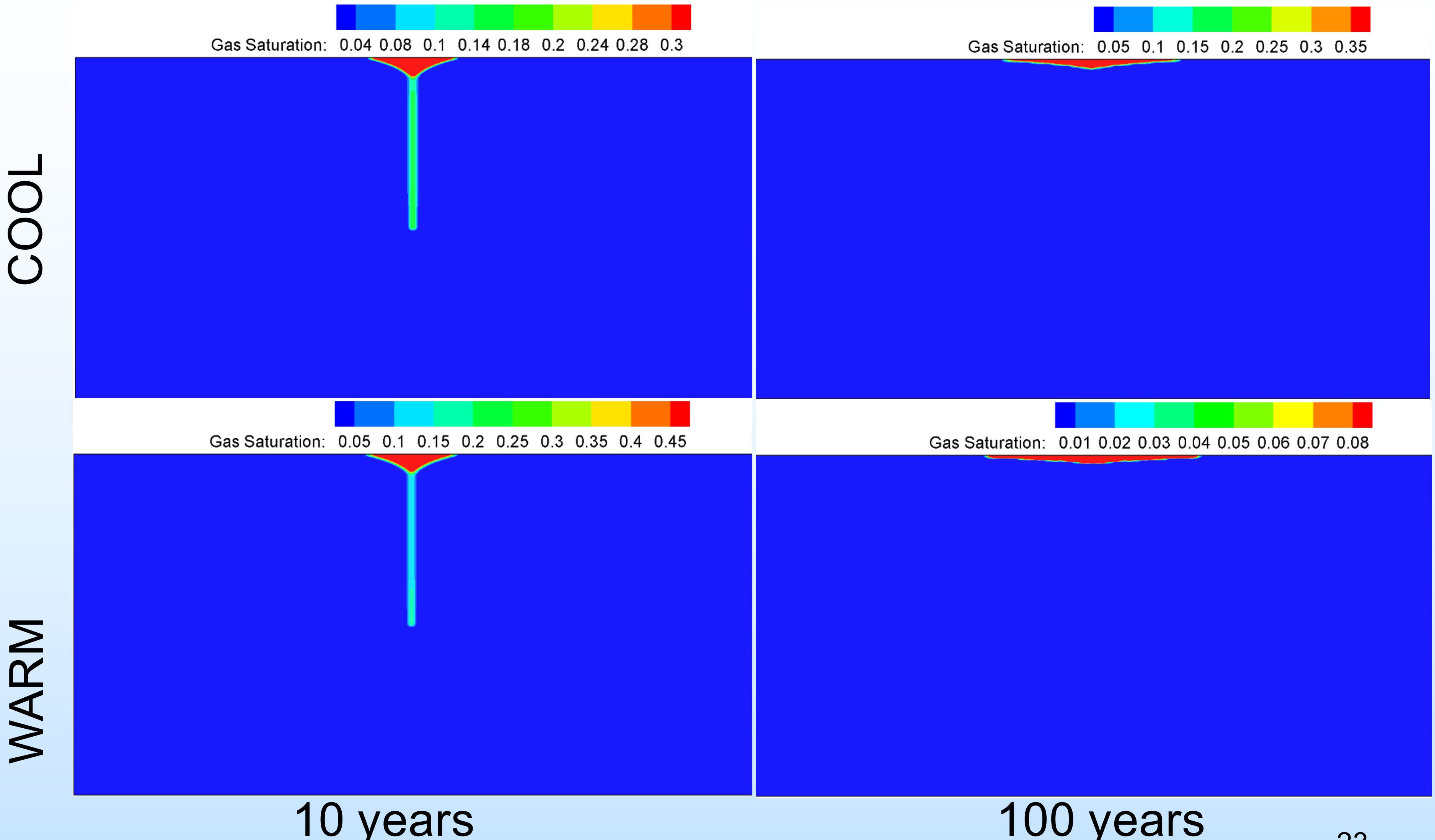

It is too shallow to develop gravity stable flow.

$scCO_2$ plumes at 3km water depth

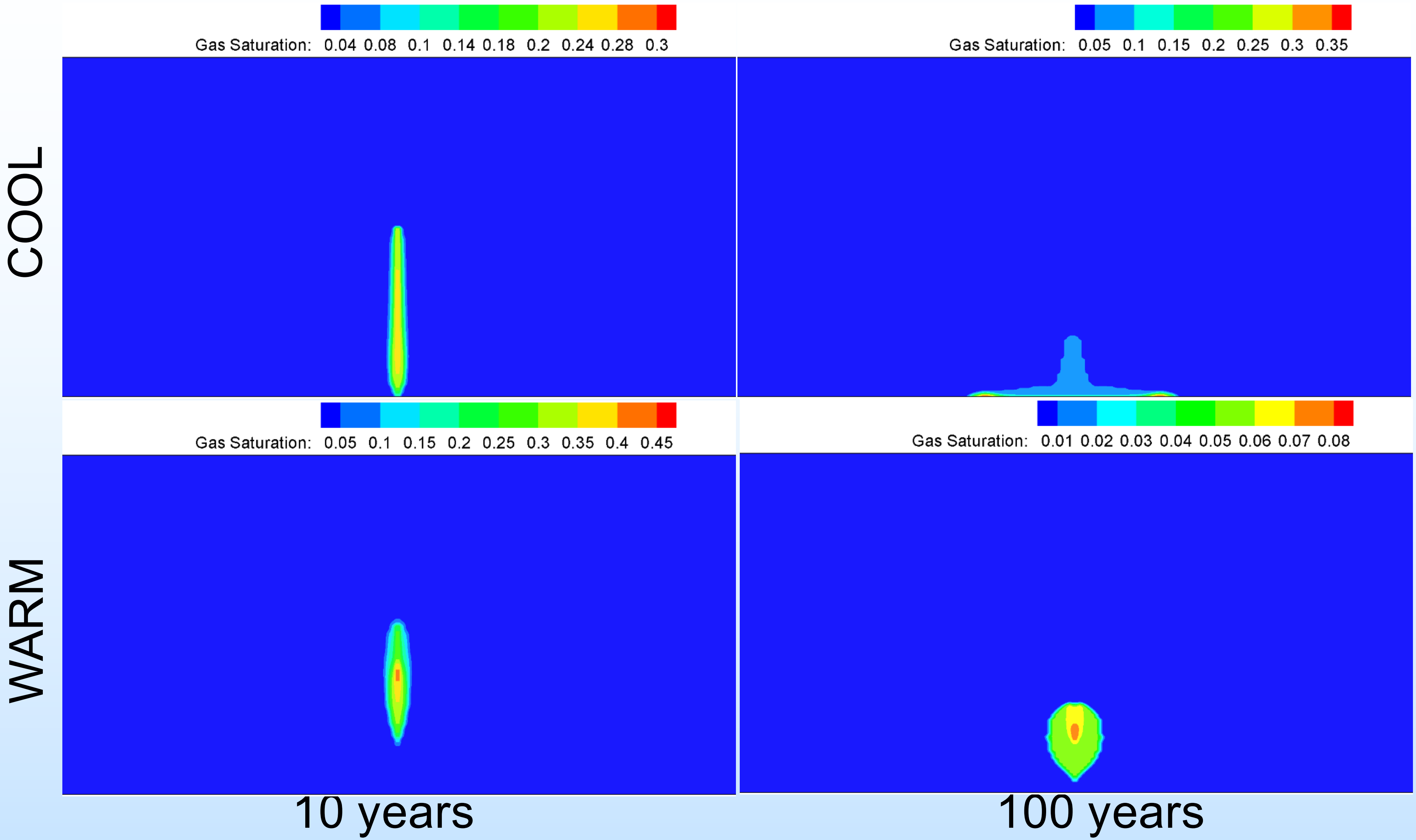

It is sufficient to develop gravity stable flow.

Dissolved CO_2 plumes at 1km water depth

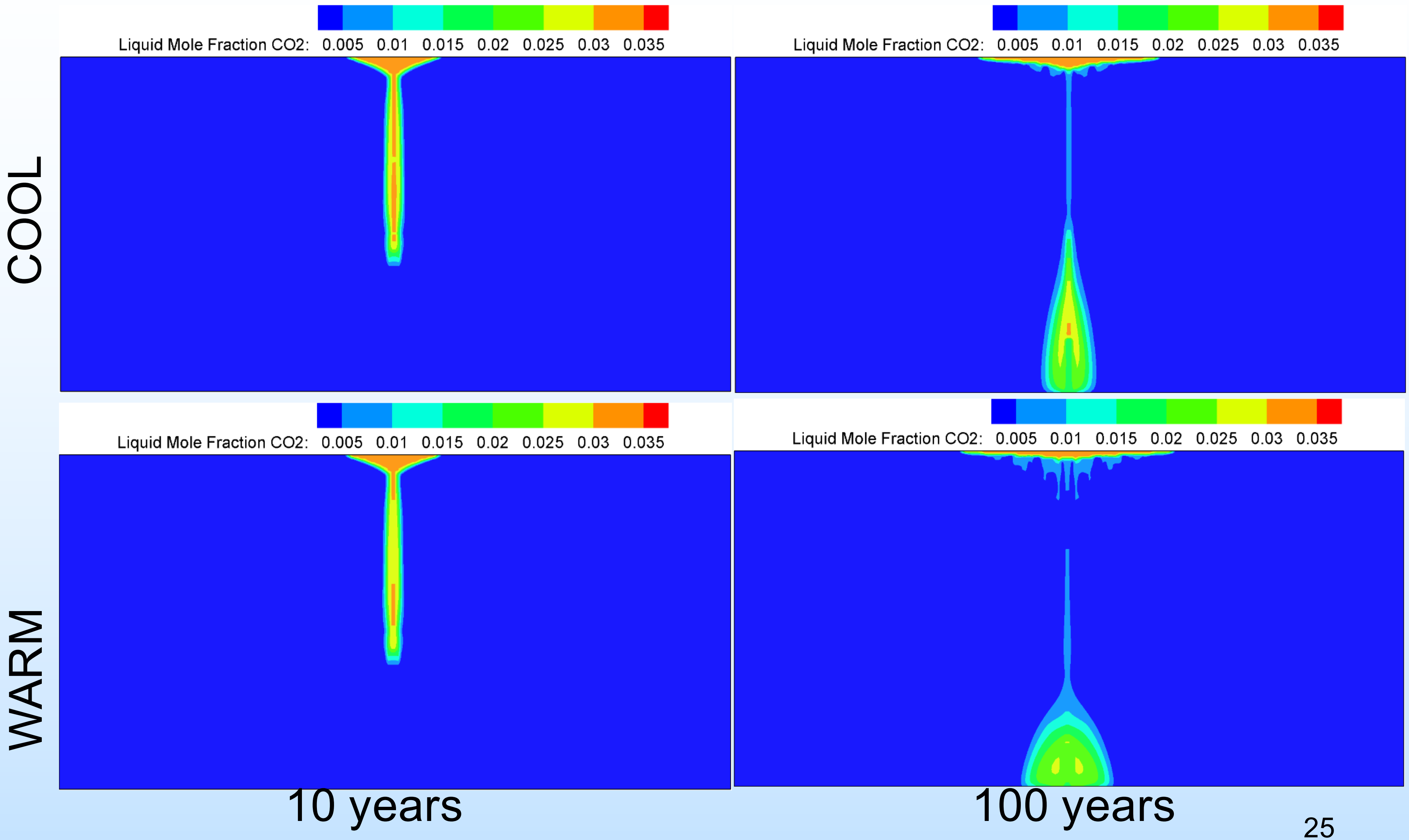

Dissolved CO_2 plumes for 3km case

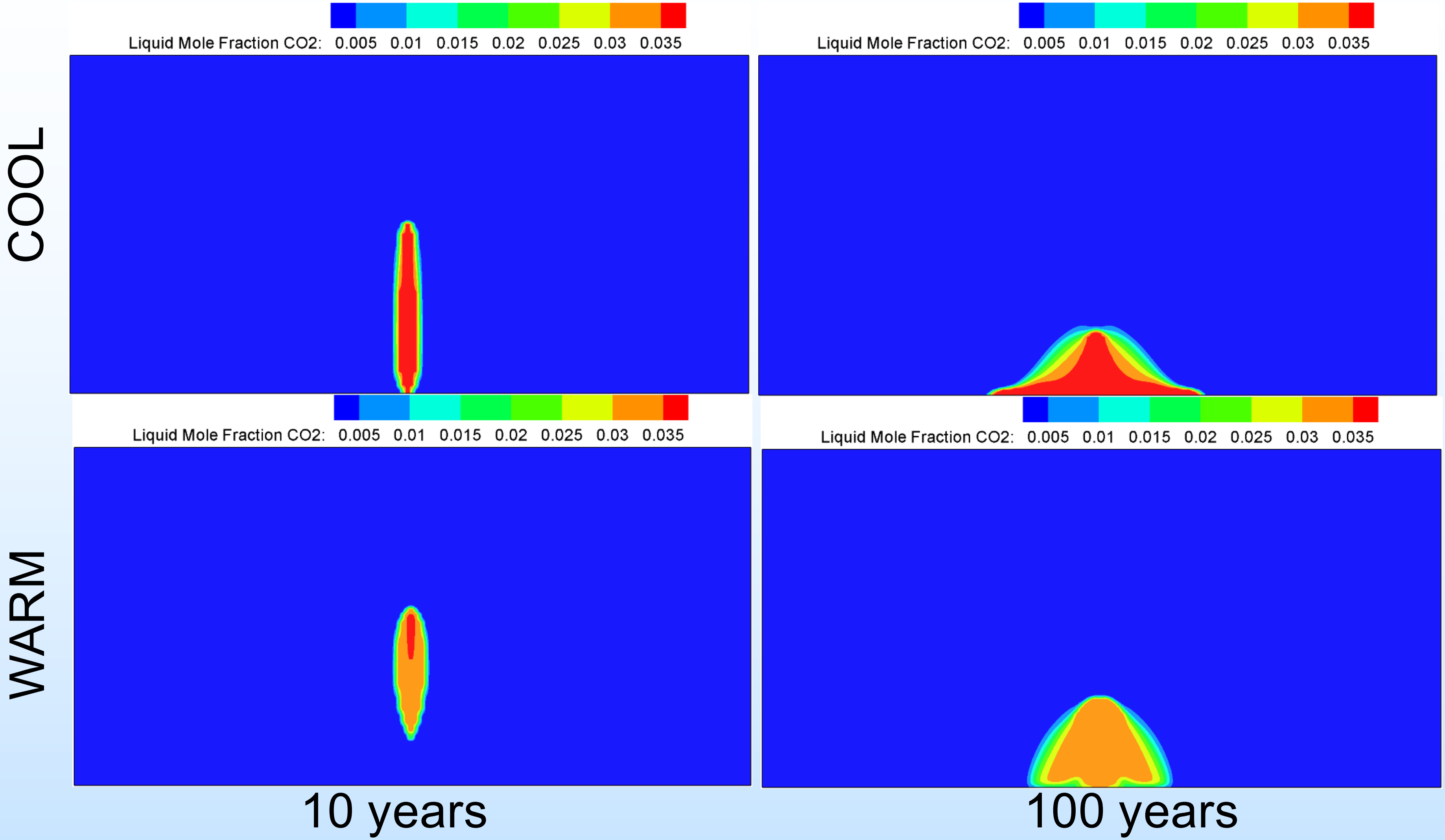

Summary

- Global upscaling computes equivalent *k*s for the geologic models with decreasing *k* resolution; for increasing reservoir ln(*k*) variances (0.1, 1.0, 4.5), FHM pressure and flow rate are captured well by the geologic models, but errors increase with variance.

- When the variance of ln(*k*) is low, the 1-unit model yields similar dissolution and leakage plumes as the FHM. When the variance of ln(*k*) is high, the 3-unit and 8-unit models provide more accurate predictions on CO_2 dissolution and leakage.

- Experimental design analysis suggests that for the uncertainty factors evaluated, brine salinity is the single most influential factor impacting CO_2 dissolution storage, while caprock permeability is the most influential factor impacting CO_2 leakage to the caprock.

- Reactions between cations and dissolved CO_2 forms carbonate mineral precipitates (i.e., Siderite and Magnesite), leading to mineral storage. High degree of uncertainty exists in its prediction.

- When the water depth is 1km, it is too shallow to develop gravity stable flow. When the water depth is 3km, it is sufficient to develop gravity stable flow. However, the magnitude of sediment permeabity can impact storage security: when $k<10^{-15}$ m^2 (clay sediment), CO_2 is also gravity neutral for all water depths, and for all geothermal gradient.

Appendix

- The following slides will not be discussed during the presentation, but are mandatory

FHM v. 1-Unit Model: σ^2_{lnk}=0.1

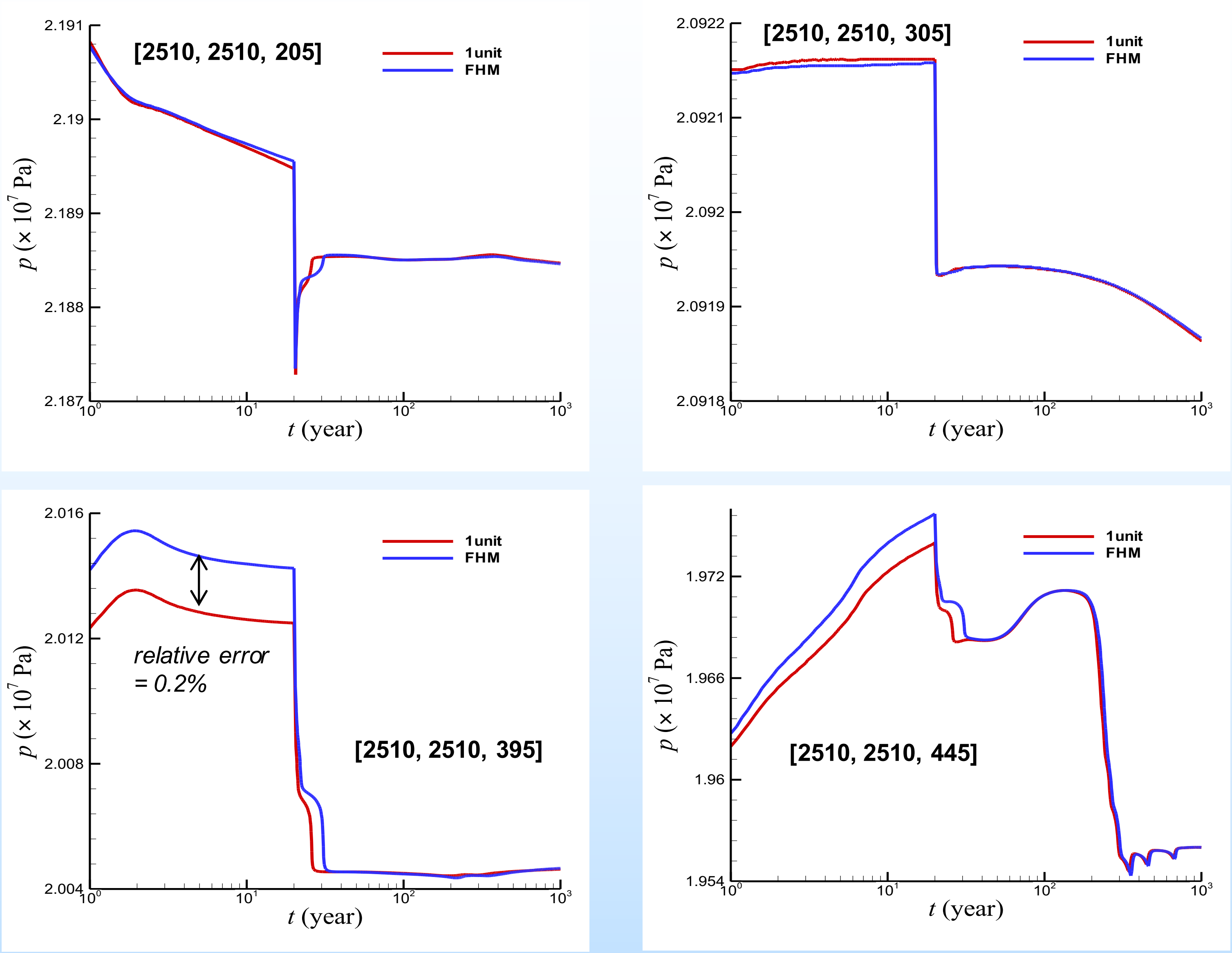

FHM v. 1-Unit Model: $\sigma^2_{\ln k}=4.5$

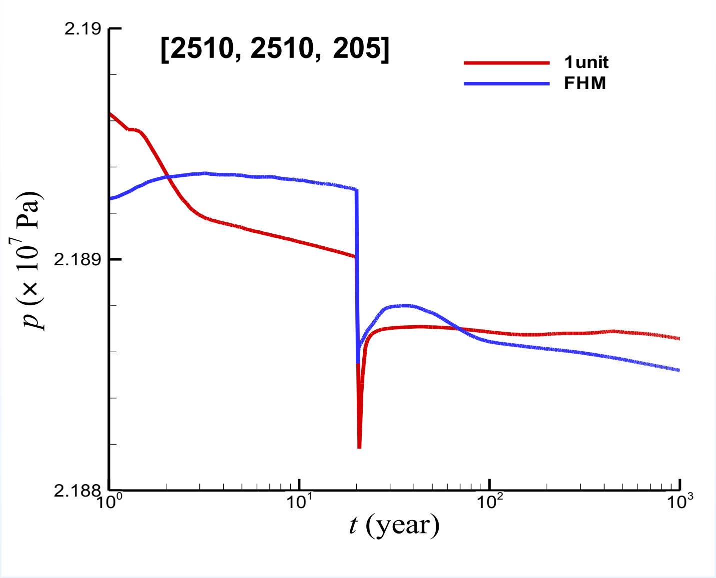

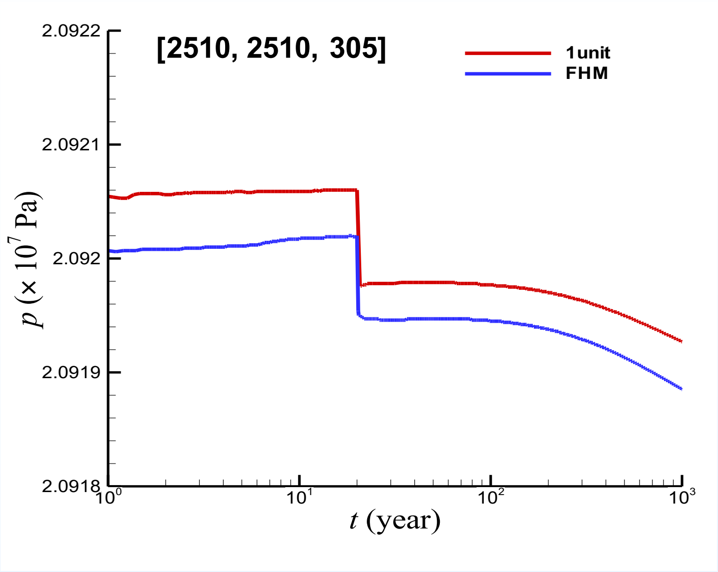

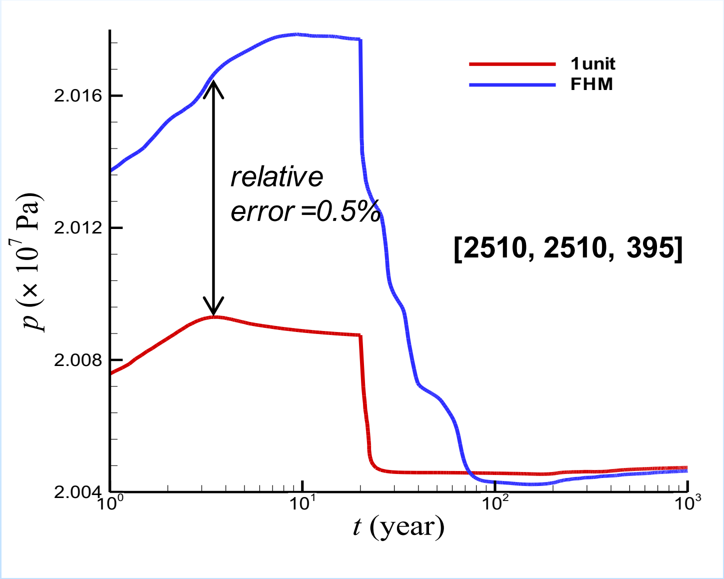

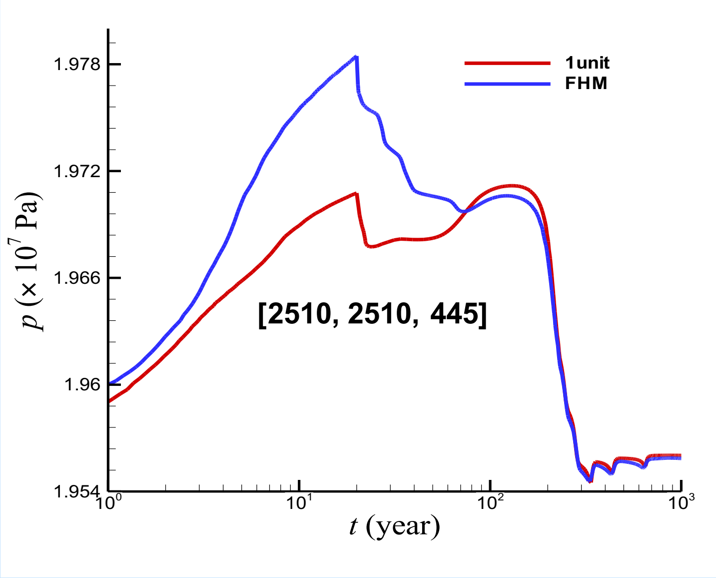

An *example 1-Unit model* run for CO_2 storage modeling simulated on the Yellowstone supercomputer. The problem domain is 7000 m x 7000 m x 250 m. Shown at 100 years for an isosurface of 0.0125 (mole fraction) of dissolved CO_2. CO_2 is injected at a depth of 50 m below the top at the center of the xy-domain for 20 years. The grid is 160 x 160 x 25 =0.64 million cells.

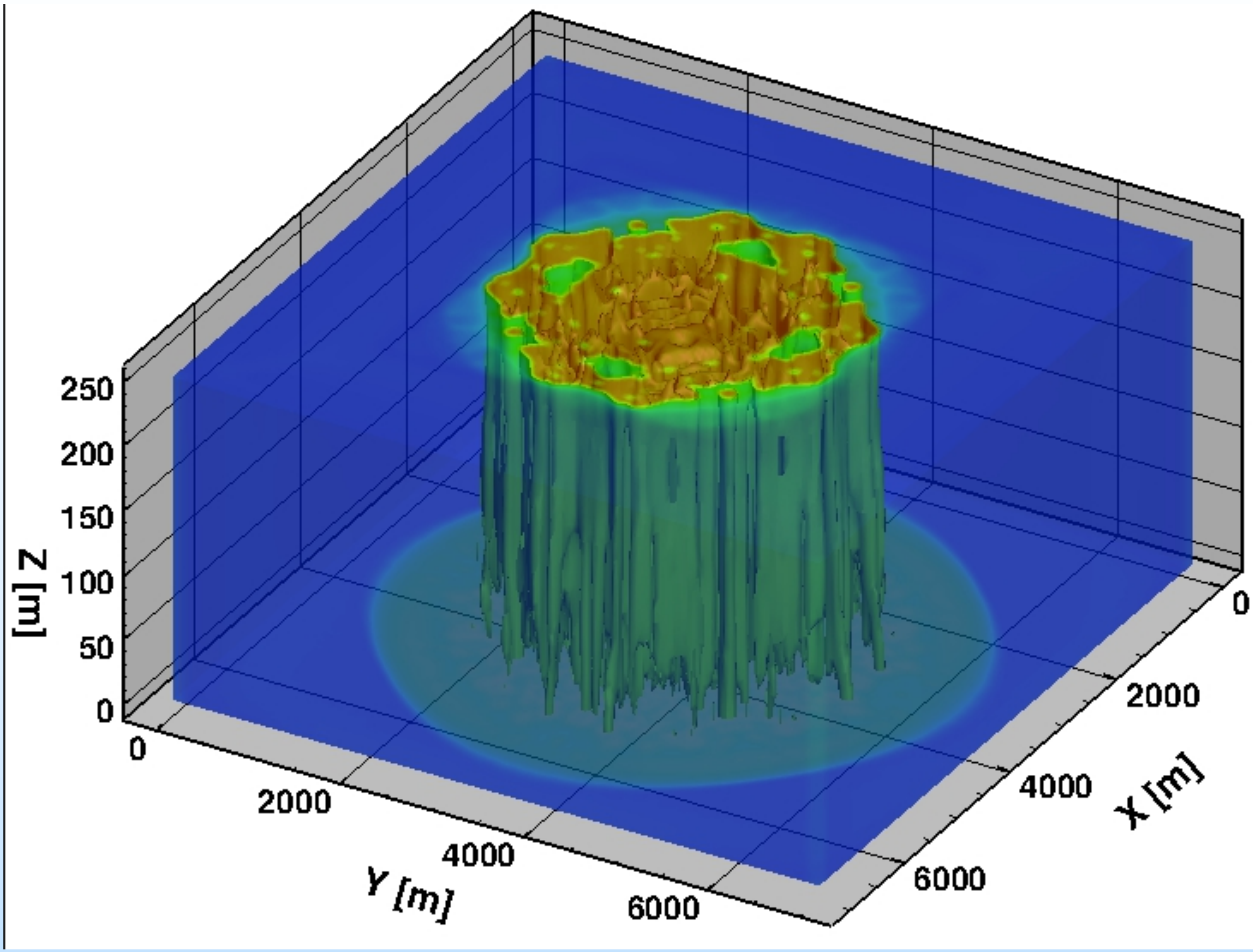

PFLOTRAN Scaling on Yellowstone

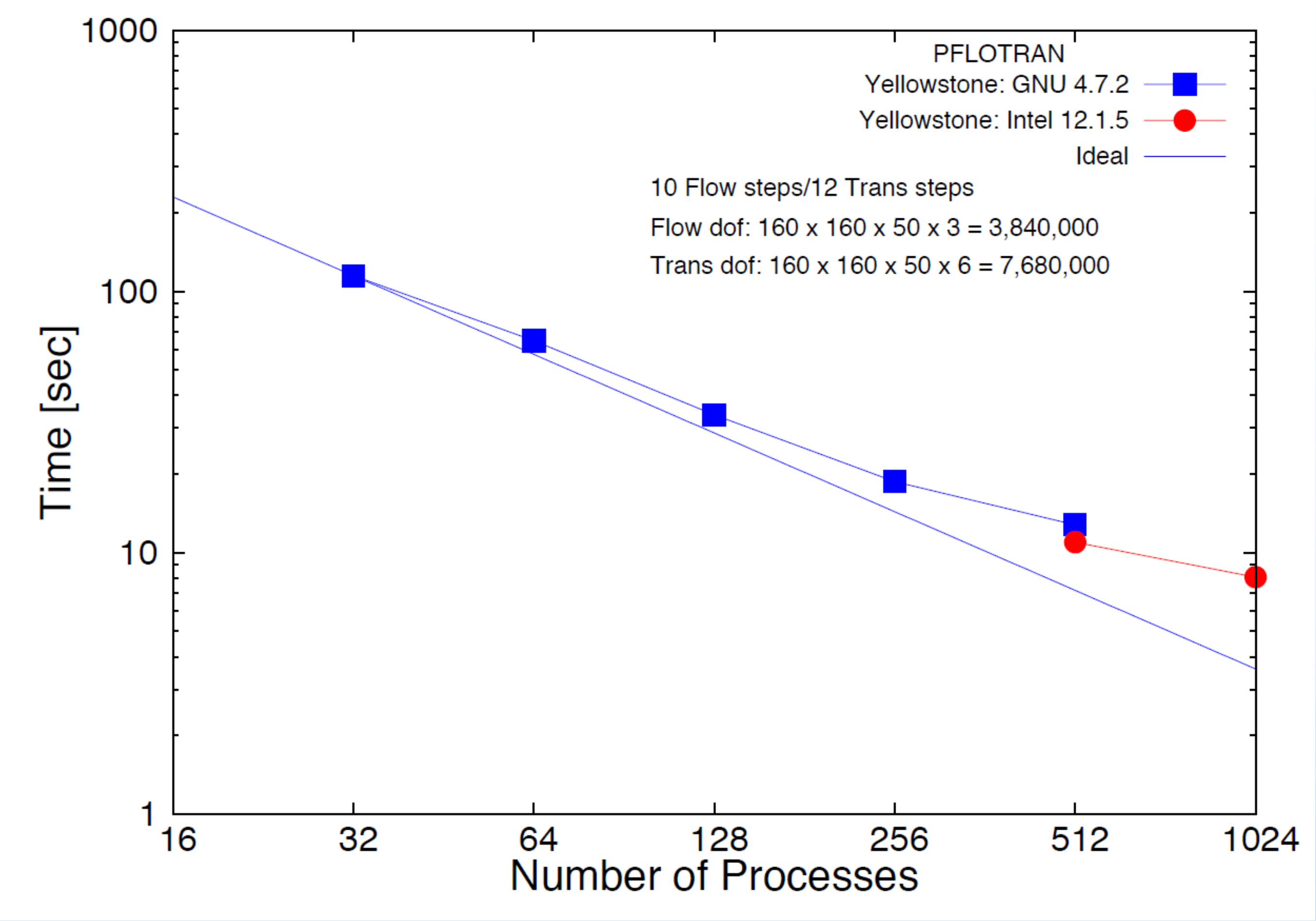

PFLOTRAN formulations

To model GCS, the following mass and energy conservation equations are solved:

$$\frac{\partial}{\partial t}\left[\varphi \sum_{\alpha}(\rho_\alpha s_\alpha X_i^\alpha)\right] + \nabla \cdot \sum_{\alpha}(\rho_\alpha X_i^\alpha \vec{q}_\alpha - \varphi \rho_\alpha s_\alpha \tau_\alpha D_\alpha \nabla X_i^\alpha) = S_i \qquad (1)$$

$$\frac{\partial}{\partial t}\left[\varphi \sum_{\alpha}(\rho_\alpha s_\alpha U_\alpha) + (1-\varphi)\rho_r C_{p,r} T\right] + \nabla \cdot \left[\sum_{\alpha}(\vec{q}_\alpha \rho_\alpha H_\alpha) - \lambda \nabla T\right] = Q \qquad (2)$$

φ denotes porosity, and $\rho_\alpha, s_\alpha, \tau_\alpha, D_\alpha, U_\alpha, H_\alpha$ refer to the density, saturation, tortuosity, diffusion coefficient, internal energy, and enthalpy of fluid phase α, respectively. Two fluid phases (CO_2, brine) will be modeled. The quantities X_i^α denote the mole fraction of component *i* in phase α. The quantities $C_{p,r}$ and λ denote the rock heat capacity and conductivity, respectively. The summation is carried out over all fluid phases present in the system. The system is assumed locally to be in thermodynamic equilibrium with temperature $T(\vec{x}; t)$ at position $\vec{x}$ and time *t*. The quantity *Q* denotes an energy source/sink term.

The quantity *Si* denotes a source/sink term for the *i*th primary species describing reaction with minerals given by $S_i = -\sum_m \nu_{im} I_m$, with stoichiometric reaction coefficients ν_{im} and kinetic rate I_m for the *m*th mineral, taken as positive for precipitation and negative for dissolution.

The flow rate $\vec{q}_\alpha$ of fluid phase α is given by the extended Darcy's law: $\vec{q}_\alpha = -\frac{\bar{\bar{k}} k_\alpha}{\mu_\alpha}(\nabla p_\alpha - \rho_\alpha g z)$, with intrinsic permeability $\bar{\bar{k}}$, relative permeability k_α, fluid viscosity μ_α, and pressure p_α of phase α.